

# On-the-Fly Machine-Learned Force Fields for High-Fidelity Polymer Glass Transition Simulations

Ashutosh Srivastava, Sakshi Agarwal, Shivank Shukla,  
Harikrishna Sahu, Rampi Ramprasad\*

School of Materials Science and Engineering, Georgia Institute of Technology, 771 Ferst Drive, Atlanta, GA 30332.

\*Corresponding author(s). E-mail(s): [ramprasad@gatech.edu](mailto:ramprasad@gatech.edu);

## Abstract

Predicting polymer glass transition temperatures ( $T_g$ ) with first-principles fidelity has long remained out of reach, as cooling multi-thousand-atom systems over a broad temperature range at acceptable rates exceeds the computational limits of ab initio molecular dynamics (AIMD). Here we employ a hybrid scheme that merges AIMD with accelerated on-the-fly (OTF) machine-learned force-field (MLFF) construction, enabling  $T_g$  prediction at quantum-mechanical accuracy with near-classical computational cost. The OTF protocol to construct MLFFs adaptively triggers first-principles calculations only when newly encountered configurations lie outside the current model's domain of confidence, allowing robust, parameter-free MLFFs to be built from merely  $\sim$ 1000 AIMD-sampled configurations per polymer. These MLFFs are then utilized to perform long-time cooling simulations on amorphous supercells containing several thousand atoms. Applied across twelve polymers spanning aromatic, aliphatic, heteroatomic, and branched chemistries, the method yields predictions in excellent accord with experiment while reducing computational cost by approximately six orders of magnitude relative to AIMD. This work establishes a new paradigm for predictive polymer modeling, demonstrating that OTF-MLFFs provide a generalizable, accurate, and scalable route to simulating the thermophysical behavior of complex disordered materials at quantum-mechanical fidelity.

**Keywords:** Machine Learning Force Field, On-the-fly AIMD Simulations, Glass Transition Temperature, Polymers

## 1 Introduction

High-fidelity simulations of complex macromolecular systems remain one of the central challenges in computational materials science. Many phenomena of practical and fundamental interest, including structural reorganizations in dense or disordered environments, thermophysical transitions, and collective fluctuations, unfold over nanoseconds or longer and involve thousands of atoms.<sup>[1–5]</sup> Polymers are emblematic of this challenge: their behavior is governed by slow configurational rearrangements, broad distributions of local environments, and pronounced dynamic heterogeneity that cannot be captured within the spatial or temporal windows accessible to conventional ab initio molecular dynamics (AIMD). Although AIMD provides unparalleled quantum-mechanical fidelity, its steep computational scaling confines simulations to small unit cells and/or short trajectories, rendering it inadequate for capturing the full physics of polymeric materials.

In recent years, machine-learned force fields (MLFFs) have emerged as a transformative pathway for accelerating atomistic simulations toward quantum accuracy. Neural-network architectures such as NequIP<sup>[6]</sup>, Allegro<sup>[7]</sup>, MACE<sup>[8]</sup>, and DeepMD<sup>[9]</sup>, along with kernel-based approaches<sup>[10, 11]</sup>, have demonstrated remarkable gains in accuracy, transferability, and scalability. However, these models generally require extensive, carefully curated training datasets and substantial computational infrastructure. These issues highlight the challenges in achieving both stability and physical fidelity in MLFF-driven polymer simulations. For polymers, where a complex hierarchy of primary and secondary interactions coexists and where configurational diversity is vast, such data demands and training burdens have impeded widespread application.

Hybrid QM/ML strategies offer an appealing alternative by invoking first-principles calculations only when needed. Among these, on-the-fly (OTF) MLFF learning stands out for its adaptivity, sample efficiency, and elimination of pre-generated training sets.<sup>[12]</sup> In the OTF-MLFF paradigm, a simulation begins with a short AIMD segment that seeds an initial MLFF. As the trajectory proceeds, a Bayesian uncertainty estimator identifies configurations insufficiently represented in the model. Only in these cases is a new first-principles calculation triggered<sup>[13]</sup>, after which the training set is expanded and the MLFF refined in real time (Figure 1(a)). As configurational diversity increases during the run, the frequency of AIMD evaluations rapidly diminishes, and the force field becomes progressively more robust. The result is a parameter-free, ready-for-use, and physically grounded MLFF that approaches AIMD accuracy (within the domain of the original simulations) while operating near-classical computational cost.

Despite these advances, predicting the glass transition temperature ( $T_g$ ) of polymers with first-principles fidelity has remained out of reach.  $T_g$  marks a fundamental thermophysical transformation, a second-order transition separating rubbery and glassy regimes, and dictates mechanical performance, thermal stability, and processability.<sup>[14–17]</sup> Accurate  $T_g$  estimation requires slow cooling from the melt, precise detection of subtle volumetric discontinuities, and ample sampling of heterogeneous dynamics, conditions that challenge the computational capabilities of

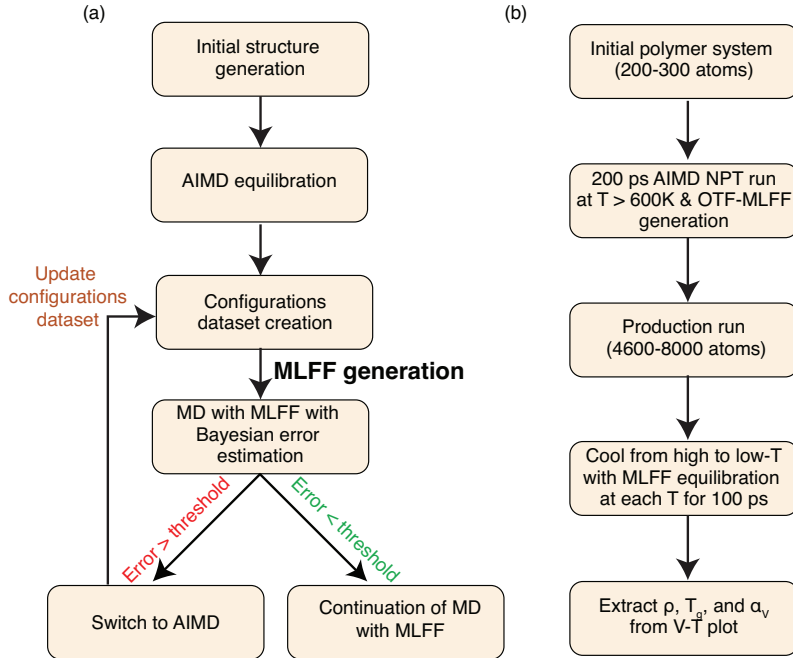


**Fig. 1** Adaptive on-the-fly machine-learning force-field (OTF-MLFF) framework for polymer thermophysical prediction. (a) Stepwise protocol for generating MLFFs, beginning with initial AIMD equilibration, Bayesian error estimation, automated dataset expansion, and real-time force-field refinement. (b) Workflow for predicting polymer glass transition temperature ( $T_g$ ) and subsequent long-time ML-driven cooling trajectories enabling high-resolution volume–temperature ( $V-T$ ) analysis to obtain density ( $\rho$ ),  $T_g$ , and volume thermal expansion coefficient ( $\alpha_v$ ).

AIMD[15, 17–19]. Classical molecular dynamics can perform long cooling trajectories but relies on empirical force fields whose transferability across polymer families, chemistries, and architectures may be unreliable or is sometimes infeasible. Recent strides in simulating the glass transition phenomenon in polymers using standalone MLFFs such as Vivace[8] and MACE-OFF[20], while promising, also highlight key challenges- likely rooted in the careful selection of the training data. These approaches either fail to reveal the glass transition with sufficient clarity or fail entirely for certain polymer chemistries (refer to supplementary figures S6 and S7 [20]).

Here, we present the first general and scalable OTF-MLFF[13, 21] framework capable of predicting polymer  $T_g$  with ab initio fidelity across a broad chemical space, enabled by the capability implemented in the *Vienna Ab-initio Simulation Package* (VASP)[22, 23]. We evaluate twelve polymers spanning aromatic, aliphatic, heteroatomic, and branched architectures. For each system, an MLFF is generated from a 200-ps NPT equilibration at elevated temperatures (600–800 K), using only  $\sim 1000$  quantum-sampled configurations. These MLFFs are then deployed to equilibrate large amorphous supercells containing several thousand atoms and to perform gradual cooling from the melt to cryogenic temperatures (Figure 1b). From the resulting volume–temperature profiles,  $T_g$ , density, and thermal expansion coefficients are

extracted. Across all polymers, the predicted quantities exhibit excellent agreement with experiment while reducing computational cost by roughly six orders of magnitude relative to a full AIMD treatment.

More broadly, this work establishes a new paradigm for predictive physics-driven polymer modeling, with quantum-mechanical accuracy delivered at near-classical computational expense. By making high-fidelity, large-scale simulations of polymers tractable on modest computational resources, this approach unlocks unprecedented opportunities to interrogate complex polymer phenomena—from segmental dynamics and viscoelasticity to diffusion, aging, mechanical behavior, and chemically triggered transformations—at speeds and scales that were inconceivable only a few years ago.

## 2 Results

**Establishing the approach using polyethylene:** In AIMD simulations, the integration time step ( $\Delta t$ ) is a critical parameter that controls both accuracy and numerical stability. Larger time steps reduce computational cost but risk significant errors in energies and forces, while smaller time steps improve fidelity at the expense of substantially higher computational effort. This balance is especially important for polymers, where high-frequency vibrational modes—dominated by C–H motions—impose stringent requirements for stability. To assess the impact of  $\Delta t$ , we developed a  $T_g$  simulation protocol using polyethylene (PE), chosen for its simplicity and well-characterized behavior. An amorphous single-chain 33-mer PE structure (composed of 206 atoms) was generated at 300 K using the Polymer Structure Predictor (PSP)[24] and subsequently equilibrated at 600 K for 200 ps using AIMD with OTF-MLFF. Density profiles were extracted for  $\Delta t$  values of 0.3, 0.4, and 0.5 fs. As shown in Figure 2(a). Detailed information on  $\Delta t$ , number of AIMD-assisted OTF-MLFF steps, configuration sampled, and CPU time has been mentioned in Figure 2(b). The 0.5 fs simulation exhibited large density fluctuations, indicating numerical instability, whereas the 0.3 and 0.4 fs simulations produced nearly identical, well-behaved density trajectories. Both yielded comparable sampling quality (1000 vs. 1002 configurations) used to create MLFF, but with a notable difference in cost: the 0.3 fs simulation required  $\sim$ 30% more wall time (96 h) than the 0.4 fs run (75 h). Balancing accuracy and efficiency, a time step of  $\Delta t = 0.4$  fs was identified as the optimal choice and was therefore used for all subsequent simulations in this study.

The local atomic environments sampled during the high-temperature equilibration were used to construct a production-ready MLFF. This MLFF was then used to calculate the  $T_g$  of the 33-mer amorphous PE structure obtained at the end of the 600 K AIMD with OTF-MLFF simulation. The system was cooled from 600 K to 50 K in 25 K decrements, equilibrating for 100 ps at each temperature. The final configuration from each step served as the starting point for the next, and the average volume was computed from the last 50 ps of each trajectory segment to ensure thermal equilibration. The resulting volume–temperature curve (Figure 2(c)) was fitted to extract the glass transition temperature, with the  $T_g$  value indicated by the dotted vertical green line. The emergence of two distinct linear regimes in the volume–temperature relationship further demonstrates the model’s ability to faithfully reproduce the second-order

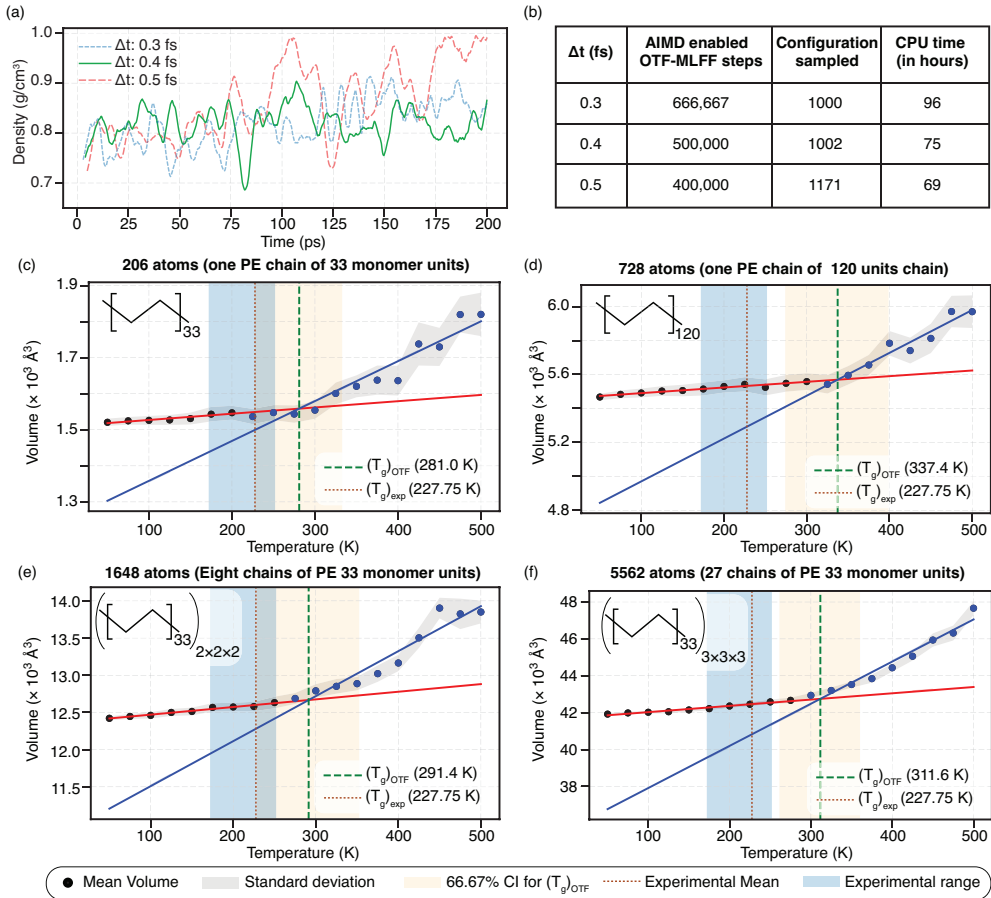


**Fig. 2** Thermodynamic behavior and computational performance of machine-learned force-field simulations across system sizes. (a) Density as a function of simulation time for different integration step sizes ( $\Delta t = 0.3, 0.4$ , and  $0.5$  fs) at 600 K. (b) Summary of timestep selection, number AIMD enabled OTF-MLFF steps required for a 200 ps trajectory, configurations sampled, and total CPU time (hours). (c–f) Volume–temperature relations for polyethylene systems containing 206, 728, 1648, and 5562 atoms constructed from multiple chains of varying lengths.

phase transition behavior characteristic of polymer glass transitions. A 66.67% confidence interval, obtained via error-propagation analysis (Supplementary Information), is shown as the orange-shaded region, while the gray-shaded regions represent the standard deviation of the volume at each temperature. The computed  $T_g$  of  $281 \pm 51.7$  K is in reasonable agreement with the experimental range reported for a variety of polyethylene flavors[25, 26], indicated by the blue-shaded region. Fluctuations in the average volume at elevated temperatures are primarily attributed to finite-size effects inherent to the 33-mer model. Nonetheless, the MLFF exhibits strong stability and transferability across the full temperature range.

**Testing scalability across system sizes:** Next, we consider PE systems with longer chain lengths and significantly larger simulation cells containing multiple

repeat units. The monomer definitions and structural details of the various amorphous PE models are provided in SI-Table 1, and the corresponding  $T_g$ -derived volume-temperature curves are shown in Figures 2(c–f). As the system size increases, the volume fluctuations during cooling diminish noticeably, yielding smoother and more stable volume-temperature profiles. This effect is particularly apparent in the 5562-atom system (Figure 2(f)), where local structural variations are averaged out more effectively, leading to a more uniform macroscopic response.

These results demonstrate that an MLFF trained on a relatively small configuration set remains robust when transferred to substantially larger systems of the same chemical composition. The model preserves accuracy and stability across both system size and temperature, underscoring the inherent scalability of the OTF-MLFF framework. Furthermore, from the  $T_g$  simulations, we extracted the coefficient of thermal expansion (CTE) in the glassy and rubbery regimes. Across all PE systems studied, the CTE ranges from  $60.5 \times 10^{-6}$  –  $113.4 \times 10^{-6} \text{ K}^{-1}$  below  $T_g$  and  $438.6 \times 10^{-6}$  –  $671.2 \times 10^{-6} \text{ K}^{-1}$  above  $T_g$ , in good agreement with the reported experimental values in the range  $\sim 93 \times 10^{-6} \text{ K}^{-1}$  –  $600 \times 10^{-6} \text{ K}^{-1}$  [26–28]. This also confirms that the MLFF not only reproduces  $T_g$  behavior but also captures the fundamental thermophysical physics associated with polymer relaxation and thermal expansion.

**Validating approach over different chemistries:** To evaluate the generality of the OTF-MLFF framework across diverse chemistries, we selected a set of polymers spanning a wide range of structural complexity and experimental  $T_g$  values. The SMILES representations[29] and molecular structures of all polymers are provided in SI-Table 2. For each system, an initial amorphous cell containing roughly 200–250 atoms was constructed using PSP; the corresponding number of monomer units and total atoms per cell are also summarized in SI-Table 2. This training system size reflects the practical computational limits of AIMD (based on the Figure 2(b) analysis), ensuring that each MLFF could be generated within a feasible wall time. Each polymer was equilibrated for 200 ps at a designated training temperature ( $T_{\text{training}}$ ), chosen to sample a broad and representative range of atomic configurations suitable for subsequent  $T_g$  simulations. The number of configurations collected during training ( $N_{\text{sampled}}$ ) varied by chemical complexity and is listed in SI-Table 2. Leveraging the insights drawn from the PE case, we then considered significantly large structures for temperature-ramped simulations, typically 4600–8000 atoms constructed by replicating and combining multiple chains of each polymer.

The resulting volume-temperature curves, shown in Figures 3(a)–(l), include the polymer structures, the standard deviation in equilibrated volumes (gray-shaded regions), and the fitted  $T_g$  values with their associated confidence intervals (vertical dashed green lines). Corresponding density-temperature plots for all cases are provided in SI-Figure 1. Across all twelve polymers studied, the predicted  $T_g$  values agree closely with the experimental values and lie within or close to the respective confidence bounds. This strong correlation underscores the predictive reliability of the OTF-MLFF approach, which successfully captures the glass transition behavior of polymers with aromatic, aliphatic, branched, and heteroatom-containing backbones. Because the entire workflow is anchored in first-principles calculations and involves

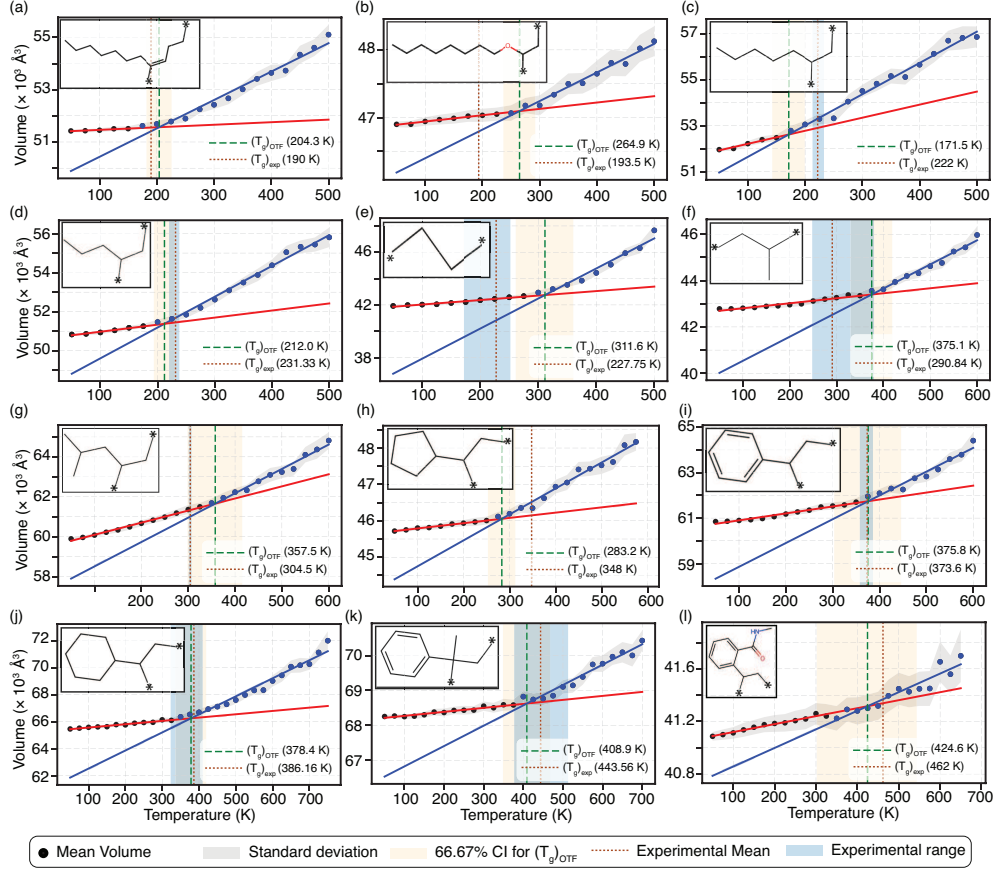


**Fig. 3** Volume–temperature behaviour of the polymers considered in this study. The corresponding polymer structures are shown in each panel. Red and blue markers with shaded gray regions denote the average volumes and standard deviations obtained from the final 50 ps of the production trajectory. Dashed green lines with shaded orange bands indicate the calculated glass-transition temperatures ( $T_g$ ) and their 66.67% confidence intervals. Experimental average  $T_g$  values are indicated by red dotted lines, and the shaded blue region indicates the experimental range of the reported  $T_g$  values for comparison.

no empirical fitting or prior knowledge of the experimental  $T_g$ , the method is inherently transferable and broadly applicable. It provides a robust and universal pathway for simulating thermophysical properties of chemically diverse polymer systems well beyond the reach of traditional force-field approaches.

The physical and chemical fidelity of the developed MLFFs is further confirmed by the excellent agreement between the predicted and experimental densities and glass transition temperatures across all polymers studied. For representative systems such as PE and polystyrene (PS), the experimental densities at 300 K of 0.88–0.93 and 1.05 g/cm<sup>3</sup>, respectively[30, 31] come close to the MLFF estimates of 0.99 and 1.09 g/cm<sup>3</sup>, respectively. Similar levels of consistency are observed for the remaining polymers, as illustrated in Figures 4(a) and (b), which compare the experimentally

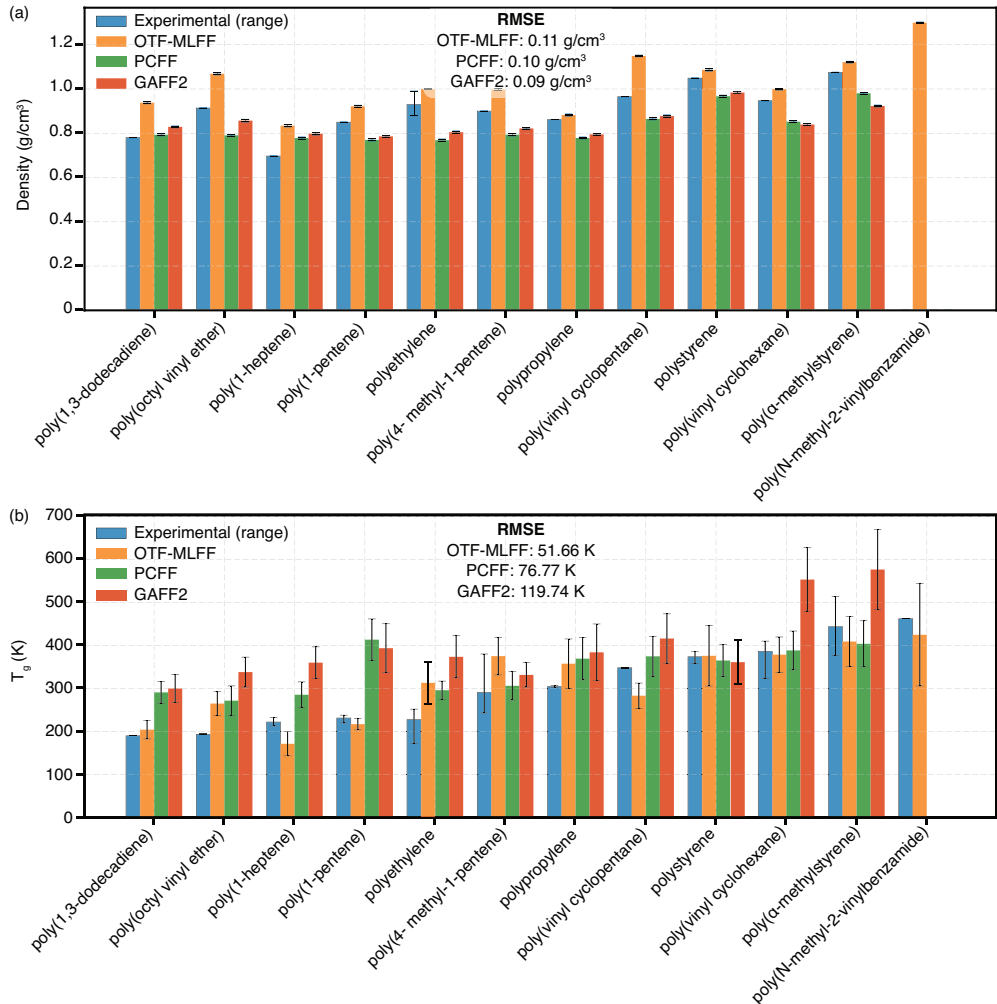


**Fig. 4** Comparison of OTF-MLFF approach predictions with reference data. (a) Densities at 300 K and (b) glass-transition temperatures ( $T_g$ ) for the polymers investigated, benchmarked against experimental measurements and classical force-field results (PCFF and GAFF2). For the last polymer (poly(N-methyl-2-vinylbenzamide)), PCFF and GAFF2 simulations were not possible due to the unavailability of classical force-field parameters.

measured and MLFF-predicted  $T_g$  values and 300 K densities. These results highlight that the OTF-MLFF workflow effectively captures the essential chemical interactions and thermophysical behavior even in systems with complex chemistries, long chain lengths, and multiple repeat units, thereby reinforcing its scalability, robustness, and versatility.

To further benchmark performance, we compared OTF-MLFF predictions with classical force-field simulations using PCFF and GAFF2. The RMSE values for density relative to experiment at room temperature are comparable across methods—0.11

$\text{g}/\text{cm}^3$  (OTF-MLFF),  $0.10 \text{ g}/\text{cm}^3$  (PCFF), and  $0.09 \text{ g}/\text{cm}^3$  (GAFF2), indicating that all three approaches reproduce equilibrium densities reasonably well at room temperature (Figure 4). In contrast, the advantage of OTF-MLFF becomes pronounced for glass-transition prediction, which is a straight test of performance over a broad temperature range: the RMSE for  $T_g$  is significantly lower at  $51.66 \text{ K}$  for OTF-MLFF, compared to  $76.77 \text{ K}$  for PCFF and  $119.74 \text{ K}$  for GAFF2. The OTF-MLFF performance also surpasses refined OPLS[32] and OPLS3e[33] force fields, which report  $T_g$  RMSE values of  $98.5 \text{ K}$ [32].

Importantly, classical force-field simulations could not be performed for poly(*N*-methyl-2-vinylbenzamide) due to missing parameters, whereas OTF-MLFF successfully handled this system without modification of the simulation protocol, reflecting its intrinsic *ab initio*-derived generality. Collectively, these comparisons underscore the ability of OTF-MLFFs to accurately capture polymer thermophysical properties even for chemistries that lie beyond the domain of traditional force fields or even stand-alone MLFFs.

### 3 Discussion

**Computational time advantage:** A notable outcome of this work is the ability of MLFFs trained on only  $\sim 1000$  AIMD configurations per polymer chemistry from 200–250-atom cells to remain accurate when applied to much larger systems. Using PE as a representative example, we now examined how the computational cost evolves with system size (Figure 5(a)). These MLFFs exhibit a near-linear (almost sublinear) scaling of  $N^{0.90}$  ( $N$  is the total number of atoms), in sharp contrast to the  $N^2$ – $N^3$  scaling of conventional DFT. This behavior highlights the practical scalability of the approach and its suitability for simulations of polymer structures containing several thousand atoms.

In order to confirm the (sub)linear scaling of the approach, the effective exponent ( $p_{\text{eff}}$ ) and time per atom ( $T/N$ ) as a function of number of atoms in the simulation ( $N$ ) were calculated.  $p_{\text{eff}}$  is extracted from two consecutive points for the two neighboring system sizes  $N_i$  and  $N_{i+1}$  with corresponding computational times  $T_i$  and  $T_{i+1}$  using the following equation:

$$p_{\text{eff}}(N_i) = \frac{\log(T_{i+1}/T_i)}{\log(N_{i+1}/N_i)} \quad (1)$$

Figure 5(b) further examines the effective scaling exponent ( $p_{\text{eff}}$ ) across system sizes. In all cases,  $p_{\text{eff}}$  remains below or close to unity, confirming sub(linear) behavior. The initial rise, followed by a gradual potential saturation close to unity, reflects the crossover from small-system overheads to the regime where the MLFF achieves its characteristic efficient scaling. A complementary assessment using the simulation time per atom (Figure 5(c)) similarly shows a monotonic decrease with increasing  $N$ . This behavior underscores both the scalability and the cost-effectiveness of the method while preserving *ab initio* accuracy for large-scale polymer simulations.

The efficiency of the approach becomes particularly evident when comparing the computational cost of  $T_g$  simulations across methods. For polyethylene, training the

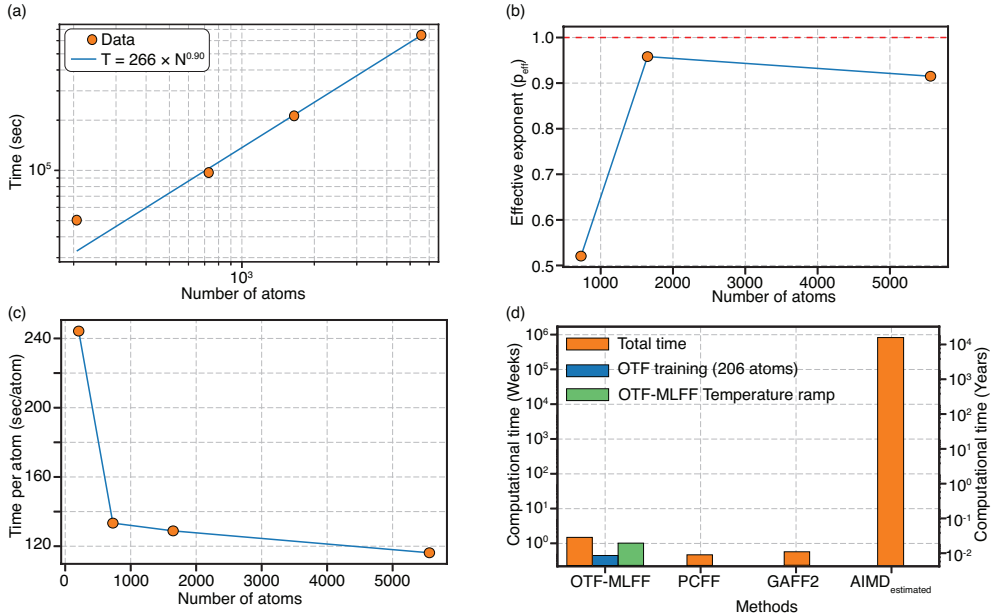


**Fig. 5** Scaling behaviour and computational benchmarking of the simulations. (a) log-log plot of simulation time with system size ( $N$ ), (b) effective exponent ( $p_{eff}$ ) as a function of  $N$ , (c) simulation time per atom versus  $N$ , and (d) Comparison of total simulation times for OTF-MLFF, the Polymer Consistent Force Field (PCFF), the General AMBER Force Field (GAFF2), and ab initio molecular dynamics (AIMD).

OTF-MLFF using a 206-atom system for 200 ps and subsequently applying it to equilibrate a 5562-atom supercell for 100 ps at 23 temperature points (from 600 K to 50 K in 25 K intervals) amounts to roughly 6.25 million simulation time-steps. Using the OTF-MLFF framework, these steps were completed in approximately 10 days on 32 cores of an *Intel(R) Xeon(R) Gold 6140 CPU @ 2.30 GHz*. The distribution of wall time between MLFF training and the  $T_g$  cooling trajectory is shown in Figure 5(d).

In stark contrast, performing the same number of simulation steps for the 5562-atom PE structure using AIMD would require an estimated  $\sim 15,000$  years on the same hardware. This estimate was determined by simply multiplying the time taken for a single time step, in the same hardware for the same system size, by 6.25 million. Given that  $T_g$  simulations inherently rely on serial cooling trajectories, such AIMD-based calculations become computationally prohibitive and likely cannot be practically scaled even on modern high-performance computing architectures. With the hybrid OTF-MLFF approach, we achieve an extraordinary speedup of approximately  $10^6$ , while preserving ab initio fidelity in energies, forces, and stresses. Importantly, this acceleration does not compromise the predictive reliability of the model, underscoring the real-world applicability of OTF-MLFF for large-scale polymer simulations and the accurate prediction of complex thermophysical properties.

**Opportunities:** While the OTF-MLFF framework is highly promising, several avenues remain for further refinement. One important direction is enhancing force-field robustness by integrating training data sampled across a broader temperature

range, which could improve transferability and performance in regimes with significant structural or dynamical variation. A temperature-diverse training strategy may reduce volume fluctuations during cooling trajectories, thereby improving the precision of  $T_g$  estimation. However, achieving this within the current VASP-based OTF workflow is computationally demanding, and the benefits relative to the required cost are not yet fully established. This challenge highlights a deeper need for algorithmic and code-level optimization, both in the underlying AIMD engine and in the MLFF construction pipeline, to reduce overheads and enable more extensive sampling. Another direction and challenge is to develop a transferable MLFF that can be created by combining previously generated OTF-MLFFs without performing new simulations. Because a model for each polymer is trained independently, differences in descriptor distributions, energy baselines, and configuration-space coverage complicate direct integration. Several computational strategies can address this limitation, including descriptor harmonization through normalization or alignment, post-hoc energy, force, and stress re-referencing to ensure consistency, and data-fusion approaches that merge and prune training sets to produce a chemically diverse yet efficient reference database. Alternatively, modular or mixture-of-experts architectures could blend multiple MLFFs based on local environments, enabling smooth interpolation across polymer chemistries. Collectively, these approaches offer a pathway toward constructing a broadly transferable, low-cost MLFF by reusing existing OTF-generated data without repeated AIMD sampling.

Looking ahead, the efficiency and near-first-principles accuracy of OTF-MLFFs open the door to entirely new classes of polymer simulations that were previously inaccessible. These include long-term thermal protocols, such as repeated cooling–heating cycles for accurate  $T_g$  prediction, as well as mechanical deformation and fracture simulations that capture bond breaking and strain localization. Additionally, molecular and ionic transport studies may be conceived that involve the diffusion of gases, solvents, and ions through dense or heterogeneous polymer matrices. OTF-MLFFs may also enable simulations of degradation mechanisms and chemical transformations. By supporting these computationally demanding studies at scale, while maintaining quantum-level fidelity, OTF-MLFFs have the potential to significantly broaden the scope of polymer modeling and provide quantitative, mechanistic insights into phenomena that have long been beyond reach.

## 4 Conclusion

In conclusion, we demonstrate that quantum-accurate simulations can be performed in a reasonable time on modest computational resources to reliably predict thermophysical phenomena, such as thermal expansion, glass transition, and density, of large disordered polymeric materials. The method is anchored on its parameter-free, first-principles foundation, combined with the acceleration capabilities of machine learning and data-efficient sampling. This allows the construction of highly accurate MLFFs from only  $\sim 1000$  sampled configurations per polymer chemistries, while avoiding exhaustive and non-essential exploration of configuration space. The resulting force fields are robust across a wide range of temperatures and chemistries—including

branched, aliphatic, heteroatomic, and aromatic polymers and scale seamlessly across system sizes without compromising on accuracy. Importantly,  $T_g$  is obtained directly from continuous cooling trajectories rather than through initialization near experimental values, reflecting the method's inherent ability to capture the transition without bias based on prior knowledge. The consistent density behavior observed in larger systems further confirms the physical reliability and transferability of the MLFFs. Together, these results establish the OTF-MLFF framework as a promising route for significantly accelerated prediction of thermophysical properties of polymeric materials and phenomena at near-first-principles accuracy.

## 5 Methods

**Structure Generation:** All the initial polymer structures were generated using an updated Polymer Structure Predictor (PSP)[24]. As the RDKit[34] often fails to generate three-dimensional (3D) structures for large or highly branched polymers, its distance-geometry-based embedding algorithm struggles to satisfy competing spatial constraints, resulting in convergence issues and steric clashes during structure generation. To address these challenges, PSP was enhanced to first construct and optimize 3D geometries of monomer and end-cap units individually, followed by their iterative assembly into polymer chains with periodic relaxation using the universal force field (UFF), thereby yielding robust and physically realistic initial geometries without embedding failures. For the construction of amorphous polymer models, PSP employs PACKMOL[35] to pack polymer chains within a simulation box while allowing rigid-body rotations and translations; however, this procedure often results in systems with densities lower than the target value. To overcome this limitation, PSP now incorporates an equilibration stage in LAMMPS[36] using the GAFF2 force field and the 21-step relaxation protocol proposed by Abbott et al.,[37], enabling efficient structural relaxation and equilibration of the amorphous models at the desired temperature.

**Molecular Dynamics Details:** The generated structures were then equilibrated, and a force-field was simultaneously trained using the OTF approach[13, 38, 39] as implemented in *Vienna Ab-initio Simulation Package* (VASP)[22, 23]. The OTF learning approach is a hybrid approach of first principles and machine learning. First-principles calculations were only executed when a new configuration was encountered for which the Bayesian error exceeds the threshold and which was not sampled earlier during the ab-initio molecular dynamics (AIMD) run.[13] Similarly, for the configurations that were very close to the configurations already sampled, the approach uses a machine learning algorithm to predict the first-principles output parameters such as forces, energies, and stresses. In this way, we collect all the distinct configurations along with the atomic positions and forces, which are then utilized to build the machine learning force field. OTF-AIMD simulations have been performed using an isothermal-isobaric (NPT) ensemble, allowing the cell shape and volume to relax during dynamics. The Langevin thermostat[40, 41] is employed to maintain temperature and pressure, utilizing the Parinello-Rahman algorithm[42, 43]. The training simulations have been performed for 200 ps (500,000 steps) with an optimized step size of 0.4

femtoseconds for polymeric structures containing lighter elements. To facilitate reasonable phase-space sampling, the initial temperature was maintained at 600 K (800 K for polymers with  $T_g \geq 400$  K), and the final temperature was set 30% higher, 780 K (1040 K). The pressure was kept at 1 atm during the run.

**Electronic Structure Calculation Details:** The plane-wave cut-off energy for the electronic charge density expression was set to 500 eV, and the overall precision of the numerical integration was set to *Accurate* to obtain reliable forces and stresses during the run. Inter-chain van-der Waals interactions were captured using the DFT-D3 scheme[44] with Becke-Johnson damping[45]. The partial electronic occupancies were treated using Fermi-smearing with a smearing width of 0.1 eV. The exchange-correlation was treated by Projector-augmented wave (PAW) pseudopotentials[46, 47] under the generalized gradient approximation (GGA). A  $1 \times 1 \times 1$   $\Gamma$ -centered  $k$ -mesh was used to sample the Brillouin zone. The electronic minimization was performed using a mixture of the blocked-Davidson and Residual Minimization Method with Direct Inversion in the Iterative Subspace (RMM-DIIS) algorithms,[48–50] with a convergence criterion of 0.00001 eV during the self-consistent loop.

**High-to-Low Temperature Cooling Details:** The constructed MLFFs for each polymer were subsequently applied to the corresponding larger polymer structures, each having ~20 to 32 polymer chains (see SI-Table 2 for details). Each system was further equilibrated using the respective MLFFs, starting from the training temperature and cooling down to 50 K in 25 K intervals. At each temperature step, simulations were run for 100 ps, and the final 50 ps of each trajectory was used to construct the volume-temperature (VT) curve. To optimize storage efficiency without compromising accuracy, volume data were recorded every ten steps and used to calculate the average and standard deviation at each temperature. The resulting VT curves were fitted with two linear segments, and the intersection point of these lines was taken as the  $T_g$  of the corresponding polymer. Additionally, an error-propagation analysis was performed to estimate the 66.67% confidence interval (CI) of  $T_g$ , based on the uncertainties in the fitted slopes (refer to the Supplementary Information for details).

**Supplementary information.** The supplementary information contains three tables having information (1) Monomer units, polymer chains, number of atoms, corresponding glass transition temperature ( $T_g$ ), and coefficient of thermal expansion of various PE structures, (2) Details of monomer units, number of atoms in the training unit cell, Number of configurations sampled during MLFF training, training temperatures, and simulated larger structure used for  $T_g$  calculations of the polymers studied in this work, and (3) OTF-MLFF estimated coefficient of thermal expansion values below and above glass transition. This section also includes a detailed description of error propagation estimation and a density-temperature plot for the simulated polymers.

**Acknowledgements.** This work is financially supported by the Office of Naval Research through a multidisciplinary university research initiative (MURI) grant N00014-20-1-2586 and the National Science Foundation through an NSF-SPEED grant 2515411. Discussions with Ayush Jain are also gratefully acknowledged.

## Declarations

- Funding
- Conflict of interest/Competing interests: The authors declare no conflict or competing interests.
- Ethics approval and consent to participate
- Consent for publication: Yes
- Data availability:
- Materials availability: Not applicable
- Code availability: Not applicable
- Author contribution: A.S. designed and established the overall simulation protocol, performed the DFT and OTF-MLFF calculations, carried out data analysis, and prepared the initial manuscript draft. S.A. contributed to the data analysis and assisted in preparing the original draft. S.S. performed the classical force-field simulations. H.S. supported the generation and preparation of polymer structures. R.R. conceived and supervised the project, provided overall guidance, and contributed to the interpretation of results.

## References

- [1] Tran, H., Gurnani, R., Kim, C., Pilania, G., Kwon, H.-K., Lively, R.P., Ramprasad, R.: Design of functional and sustainable polymers assisted by artificial intelligence. *Nat. Rev. Mater.* **9**(12), 866–886 (2024) <https://doi.org/10.1038/s41578-024-00708-8>
- [2] Muench, S., Wild, A., Fribe, C., Häupler, B., Janoschka, T., Schubert, U.S.: Polymer-based organic batteries. *Chem. Rev.* **116**(16), 9438–9484 (2016) <https://doi.org/10.1021/acs.chemrev.6b00070>
- [3] Hager, M.D., Bode, S., Weber, C., Schubert, U.S.: Shape memory polymers: Past, present and future developments. *Progress in Polymer Science* **49–50**, 3–33 (2015) <https://doi.org/10.1016/j.progpolymsci.2015.04.002>
- [4] Huan, T.D., Boggs, S., Teyssedre, G., Laurent, C., Cakmak, M., Kumar, S., Ramprasad, R.: Advanced polymeric dielectrics for high energy density applications. *Progress in Materials Science* **83**, 236–269 (2016) <https://doi.org/10.1016/j.pmatsci.2016.05.001>
- [5] Pan, M., Pan, C., Li, C., Zhao, J.: A review of membranes in proton exchange membrane fuel cells: Transport phenomena, performance and durability. *Renewable and Sustainable Energy Reviews* **141**, 110771 (2021) <https://doi.org/10.1016/j.rser.2021.110771>
- [6] Batzner, S., Musaelian, A., Sun, L., Geiger, M., Mailoa, J.P., Kornbluth, M., Molinari, N., Smidt, T.E., Kozinsky, B.: E(3)-equivariant graph neural networks for data-efficient and accurate interatomic potentials. *Nat. Commun.* **13**(1) (2022) <https://doi.org/10.1038/s41467-022-29939-5>

[7] Musaelian, A., Batzner, S., Johansson, A., Sun, L., Owen, C.J., Kornbluth, M., Kozinsky, B.: Learning local equivariant representations for large-scale atomistic dynamics. *Nat. Commun.* **14**(1) (2023) <https://doi.org/10.1038/s41467-023-36329-y>

[8] Kovács, D.P., Moore, J.H., Browning, N.J., Batatia, I., Horton, J.T., Pu, Y., Kapil, V., Witt, W.C., Magdău, I.-B., Cole, D.J., Csányi, G.: Mace-off: Short-range transferable machine learning force fields for organic molecules. *J. Am. Chem. Soc.* **147**(21), 17598–17611 (2025) <https://doi.org/10.1021/jacs.4c07099>

[9] Qi, Y., Gong, W., Yan, Q.: Bridging deep learning force fields and electronic structures with a physics-informed approach. *npj Comput. Mater.* **11**(1) (2025) <https://doi.org/10.1038/s41524-025-01668-5>

[10] Rezaei, M., Montaseri, M., Mostafaei, S., Taheri, M.: Application of kernel-based learning algorithms in survival analysis: A systematic review (2023) <https://doi.org/10.21203/rs.3.rs-2655631/v1>

[11] Müller, K.-R., Mika, S., Tsuda, K., Schölkopf, K.: An introduction to kernel-based learning algorithms. In: *Handbook of Neural Network Signal Processing*, pp. 4–1. CRC Press, ??? (2018)

[12] Botu, V., Ramprasad, R.: Adaptive machine learning framework to accelerate ab initio molecular dynamics. *Int. J. Quant. Chem.* **115**(16), 1074–1083 (2014) <https://doi.org/10.1002/qua.24836>

[13] Jinnouchi, R., Karsai, F., Kresse, G.: On-the-fly machine learning force field generation: Application to melting points. *Phys. Rev. B* **100**(1) (2019) <https://doi.org/10.1103/physrevb.100.014105>

[14] Roos, Y.H.: Glass transition temperature and its relevance in food processing. *Annual Review of Food Science and Technology* **1**(1), 469–496 (2010) <https://doi.org/10.1146/annurev.food.102308.124139>

[15] Han, J., Gee, R.H., Boyd, R.H.: Glass transition temperatures of polymers from molecular dynamics simulations. *Macromolecules* **27**(26), 7781–7784 (1994)

[16] Park, J.-M., Park, C.S., Kwak, S.K., Sun, J.-Y.: Glass transition temperature as a unified parameter to design self-healable elastomers. *Sci. Adv.* **10**(28) (2024) <https://doi.org/10.1126/sciadv.adp0729>

[17] Yu, K.-q., Li, Z.-s., Sun, J.: Polymer structures and glass transition: A molecular dynamics simulation study. *Macromolecular theory and simulations* **10**(6), 624–633 (2001)

[18] Buchholz, J., Paul, W., Varnik, F., Binder, K.: Cooling rate dependence of the glass transition temperature of polymer melts: Molecular dynamics study. *The*

Journal of chemical physics **117**(15), 7364–7372 (2002)

- [19] Mohammadi, M., Davoodi, J., *et al.*: The glass transition temperature of pmma: A molecular dynamics study and comparison of various determination methods. European Polymer Journal **91**, 121–133 (2017)
- [20] Simm, G.N.C., Hélie, J., Schulz, H., Chen, Y., Simeon, G., Kuzina, A., Martinez-Baez, E., Gasparotto, P., Tocci, G., Chen, C., Li, Y., Cheng, L., Wang, Z., Nguyen, B.H., Smith, J.A., Sun, L.: SimPoly: Simulation of Polymers with Machine Learning Force Fields Derived from First Principles. arXiv (2025). <https://doi.org/10.48550/ARXIV.2510.13696> . <https://arxiv.org/abs/2510.13696>
- [21] Vandermause, J., Torrisi, S.B., Batzner, S., Xie, Y., Sun, L., Kolpak, A.M., Kozinsky, B.: On-the-fly active learning of interpretable bayesian force fields for atomistic rare events. npj Computational Materials **6**(1), 20 (2020)
- [22] Kresse, G., Furthmüller, J.: Efficient iterative schemes for ab initio total-energy calculations using a plane-wave basis set. Phys. Rev. B **54**(16), 11169 (1996) <https://doi.org/10.1103/physrevb.54.11169>
- [23] Kresse, G., Furthmüller, J.: Efficiency of ab-initio total energy calculations for metals and semiconductors using a plane-wave basis set. Comput. Mater. Sci. **6**(1), 15–50 (1996) [https://doi.org/10.1016/0927-0256\(96\)00008-0](https://doi.org/10.1016/0927-0256(96)00008-0)
- [24] Sahu, H., Shen, K.-H., Montoya, J.H., Tran, H., Ramprasad, R.: Polymer structure predictor (psp): A python toolkit for predicting atomic-level structural models for a range of polymer geometries. J. Chem. Theory Comput. **18**(4), 2737–2748 (2022) <https://doi.org/10.1021/acs.jctc.2c00022>
- [25] Fakirov, S., Krasteva, B.: On the glass transition temperature of polyethylene as revealed by microhardness measurements. J. Macromol. Sci. Part B Phys. **39**(2), 297–301 (2000)
- [26] Ohlberg, S.M., Fenstermaker, S.S.: The determination of the glass transition temperature of polyethylene by x-ray diffraction. J. Polym. Sci. **32**(125), 514–516 (1958) <https://doi.org/10.1002/pol.1958.1203212521>
- [27] Passive-Components.eu: Coefficient of Linear Thermal Expansion on Polymers Explained. Accessed: 2025-11-29. <https://passive-components.eu/coefficient-of-linear-thermal-expansion-on-polymers-explained/>
- [28] Material Property Tables: PE (LDPE/HDPE). Accessed: 2025-11-29 (n.d.). [https://plastecprofiles.com/uploads/1/3/0/4/13043900/material\\_property\\_tables\\_pe.pdf](https://plastecprofiles.com/uploads/1/3/0/4/13043900/material_property_tables_pe.pdf)

[29] Weininger, D.: Smiles, a chemical language and information system. 1. introduction to methodology and encoding rules. *J. Chem. Inf. Comput. Sci.* **28**(1), 31–36 (1988) <https://doi.org/10.1021/ci00057a005>

[30] Cheremisinoff, N.P.: P, pp. 200–255. Elsevier, ??? (2001). <https://doi.org/10.1016/b978-0-08-050282-3.50021-4> <http://dx.doi.org/10.1016/B978-0-08-050282-3.50021-4>

[31] Gehlsen, M.D., Weimann, P.A., Bates, F.S., Harville, S., Mays, J.W., Wignall, G.D.: Synthesis and characterization of poly(vinylcyclohexane) derivatives. *J. Polym. Sci. B Polym. Phys.* **33**(10), 1527–1536 (1995) <https://doi.org/10.1002/polb.1995.090331010>

[32] Afzal, M.A.F., Browning, A.R., Goldberg, A., Halls, M.D., Gavartin, J.L., Morisato, T., Hughes, T.F., Giesen, D.J., Goose, J.E.: High-throughput molecular dynamics simulations and validation of thermophysical properties of polymers for various applications. *ACS Appl. Polym. Mater.* **3**(2), 620–630 (2020) <https://doi.org/10.1021/acsapm.0c00524>

[33] Roos, K., Wu, C., Damm, W., Reboul, M., Stevenson, J.M., Lu, C., Dahlgren, M.K., Mondal, S., Chen, W., Wang, L., Abel, R., Friesner, R.A., Harder, E.D.: Opls3e: Extending force field coverage for drug-like small molecules. *J. Chem. Theory Comput.* **15**(3), 1863–1874 (2019) <https://doi.org/10.1021/acs.jctc.8b01026>

[34] Landrum, G., et al.: RDKit: Open-Source Cheminformatics Software. <https://doi.org/10.5281/zenodo.8382820> . <https://www.rdkit.org>

[35] Martínez, L., Andrade, R., Birgin, E.G., Martínez, J.M.: Packmol: A package for building initial configurations for molecular dynamics simulations. *J. Comput. Chem.* **30**(13), 2157–2164 (2009) <https://doi.org/10.1002/jcc.21224>

[36] Plimpton, S.: Fast parallel algorithms for short-range molecular dynamics. *Journal of Computational Physics* **117**(1), 1–19 (1995) <https://doi.org/10.1006/jcph.1995.1039>

[37] Abbott, L.J., Hart, K.E., Colina, C.M.: Polymatic: a generalized simulated polymerization algorithm for amorphous polymers. *Theor. Chem. Acc.* **132**(3) (2013) <https://doi.org/10.1007/s00214-013-1334-z>

[38] Jinnouchi, R., Lahnsteiner, J., Karsai, F., Kresse, G., Bokdam, M.: Phase transitions of hybrid perovskites simulated by machine-learning force fields trained on the fly with bayesian inference. *Phys. Rev. Lett.* **122**(22) (2019) <https://doi.org/10.1103/physrevlett.122.225701>

[39] Jinnouchi, R., Karsai, F., Verdi, C., Asahi, R., Kresse, G.: Descriptors representing two- and three-body atomic distributions and their effects on the

accuracy of machine-learned inter-atomic potentials. *J. Chem. Phys.* **152**(23) (2020) <https://doi.org/10.1063/5.0009491>

- [40] Hoover, W.G., Ladd, A.J.C., Moran, B.: High-strain-rate plastic flow studied via nonequilibrium molecular dynamics. *Phys. Rev. Lett.* **48**(26), 1818–1820 (1982) <https://doi.org/10.1103/physrevlett.48.1818>
- [41] Evans, D.J.: Computer “experiment” for nonlinear thermodynamics of couette flow. *J. Chem. Phys.* **78**(6), 3297–3302 (1983) <https://doi.org/10.1063/1.445195>
- [42] Parrinello, M., Rahman, A.: Crystal structure and pair potentials: A molecular-dynamics study. *Phys. Rev. Lett.* **45**(14), 1196–1199 (1980) <https://doi.org/10.1103/physrevlett.45.1196>
- [43] Parrinello, M., Rahman, A.: Polymorphic transitions in single crystals: A new molecular dynamics method. *J. Appl. Phys.* **52**(12), 7182–7190 (1981) <https://doi.org/10.1063/1.328693>
- [44] Grimme, S., Antony, J., Ehrlich, S., Krieg, H.: A consistent and accurate ab initio parametrization of density functional dispersion correction (dft-d) for the 94 elements h-pu. *J. Chem. Phys.* **132**(15), 154104 (2010) <https://doi.org/10.1063/1.3382344>
- [45] Grimme, S., Ehrlich, S., Goerigk, L.: Effect of the damping function in dispersion corrected density functional theory. *J. Comput. Chem.* **32**(7), 1456–1465 (2011) <https://doi.org/10.1002/jcc.21759>
- [46] Blöchl, P.E.: Projector augmented-wave method. *Phys. Rev. B* **50**(24), 17953 (1994) <https://doi.org/10.1103/physrevb.50.17953>
- [47] Kresse, G., Joubert, D.: From ultrasoft pseudopotentials to the projector augmented-wave method. *Phys. Rev. B* **59**(3), 1758 (1999) <https://doi.org/10.1103/physrevb.59.1758>
- [48] Kresse, G., Furthmüller, J.: Efficiency of ab-initio total energy calculations for metals and semiconductors using a plane-wave basis set. *Comput. Mater. Sci.* **6**(1), 15–50 (1996) [https://doi.org/10.1016/0927-0256\(96\)00008-0](https://doi.org/10.1016/0927-0256(96)00008-0)
- [49] Kresse, G., Furthmüller, J.: Efficient iterative schemes for ab initio total-energy calculations using a plane-wave basis set. *Phys. Rev. B* **54**(16), 11169–11186 (1996) <https://doi.org/10.1103/physrevb.54.11169>
- [50] Pulay, P.: Convergence acceleration of iterative sequences. the case of scf iteration. *Chem. Phys. Lett.* **73**(2), 393–398 (1980) [https://doi.org/10.1016/0009-2614\(80\)80396-4](https://doi.org/10.1016/0009-2614(80)80396-4)